Accepted for presentation in: 2023 IEEE 97th Vehicular Technology Conference (VTC-Spring), Florence, Italy, June 2023.

Characterization of 5G mmWave High-Accuracy Positioning Services for Urban Road Traffic

Simon Häger, Niklas Gratza, and Christian Wietfeld
Communication Networks Institute (CNI), TU Dortmund University, 44227 Dortmund, Germany
E-mail: {Simon.Haeger, Niklas.Gratza, Christian.Wietfeld}@tu-dortmund.de

***Abstract*—The ongoing development towards autonomous traffic requires detailed context information, including highly accurate position estimates. The 5G standard has therefore extended its feature support for positioning and defined six service levels (SLs) to cater to the various commercial use cases. User positioning at millimeter-waves (mmWaves) is considered particularly promising due to the inherent support for angle measurements and the contiguous broad bands. However, in the literature, a comprehensive classification of the achievable SLs with different positioning algorithms under different parameter measurement errors is missing. Based on ray-tracing data, we find that only the lower SLs can be achieved in an urban scenario, whereas SLs 4 to 6 are hard to meet due to the high availability requirements. For such use cases, hybrid positioning is needed to shorten the tail of the error distribution further: We show that positioning with a single base station (BS) is particularly well-suited because the identified network time synchronization problem is bypassed, thus attaining high accuracy at low overhead. Service availability can be improved further by integrating satellite-based estimates.**

I. Introduction

Basic positioning capabilities in cellular networks have been introduced decades ago for regulatory services and extended steadily since [1]. The initial 5G release, i.e., release 15, adopted the latest capabilities of 4G networks. Recently, rel. 16 enhanced the positioning support which is set to be evolved even further by rels. 17 to 18. The aim of 5G rel. 16 and beyond location services (LCSs) is to offer enhanced capabilities enabling commercial and industrial use cases such as localization and tracking of pedestrians, vehicles, and assets in challenging environments, e.g., indoor industrial facilities or busy urban outdoor environments [2]. Moreover, there is also interest in network-internal usage, e.g., for location-aware handover increasing the robustness of 5G and future 6G communication [3]. Thus, precise positioning can be seen as a key factor and enabling technology of intelligent transportation systems (ITSs) as depicted in Fig. 1.

The required positioning quality of service (QoS) metrics depend on the given use case. As of now, the Third Generation Partnership Project (3GPP) standardization has defined seven SLs with the strongest requirements, for example, demanding dm-level horizontal accuracy compared to the latest 4G network's accuracy in the tens of meters [4]. To meet such ambitious requirements, the wider bands and large-scale antenna arrays employed in 5G mmWave networks shall offer the necessary degrees of freedom enabling highly accurate positioning with time and angle information-based techniques at reduced multipath-based distortions at mmWaves.

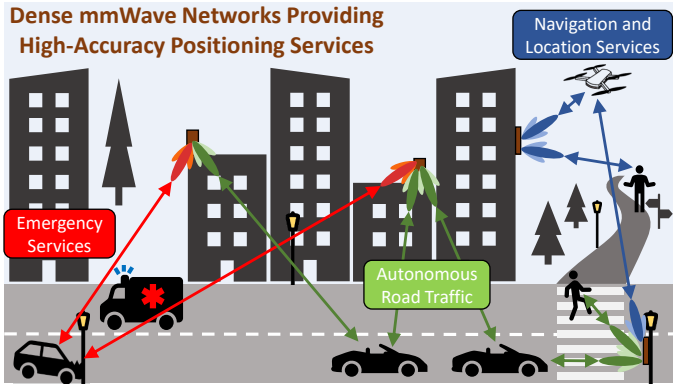

Fig. 1. 5G positioning services enable future ITS use cases [5], [6]. Dense mmWave deployments offer high accuracy via fine angular information from the antenna arrays and precise time measurements by using broad bandwidths.

Whereas there are numerous works on 5G and mmWave positioning, with the annual number of related publications rising, there is an insufficient characterization of which 3GPP positioning SLs can be attained by dense urban deployments. In addition, existing work is not comprehensive enough in terms of the size of the dataset, the error assumptions, and the positioning techniques used. Therefore, this work aims to fill this gap by a comprehensive classification of outdoor mmWave positioning capabilities with a focus on horizontal accuracy requirements. The results shall be transferred into 6G research.

The remainder of this paper is structured as follows: Referring to related work, Sec. II provides a brief overview of 5G positioning standardization and the current state of research within the field of 5G mmWave-based positioning. Afterward, Sec. III elaborates on the implemented and proposed user positioning techniques, the urban mmWave ray-tracing scenario, and error modeling. Sec. IV contains the evaluation of the attained mmWave positioning performance. Last, a summary of our key findings concludes this work.

II. Overview of 5G Positioning

This section provides an overview of 5G positioning. In Sec. II-A we lay out the novelties of 5G rels. 16 and beyond designed to meet the high requirements discussed in Sec. II-B. Last, Sec. II-C discusses current related research works.

A. 5G Positioning: Signals, Measurements, and Estimation

Similar to 4G, the 5G positioning architecture evolves around the Location Management Function (LMF) in the

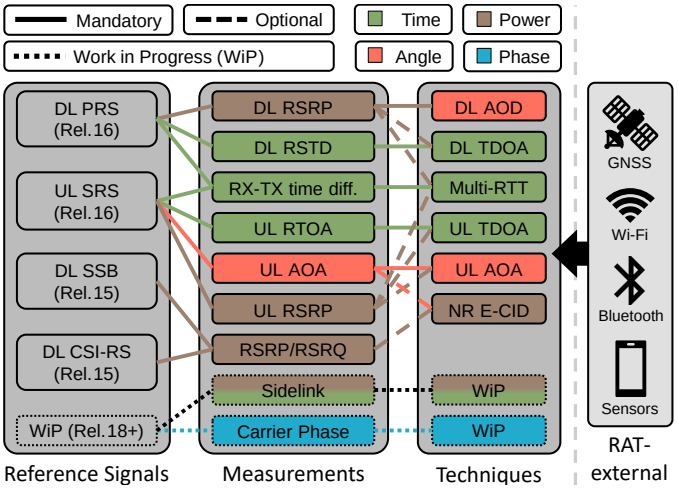

Fig. 2. Compact overview of standardized and expected signals, measurements, and positioning techniques for 5G and beyond networks [7], [10], [11].

core network. An overview of the radio access technology (RAT)-internal user positioning capabilities of 5G is given in Fig. 2 and explained subsequently. The LMF uses up to four reference signals to collect assistive data, i.e., via downlink (DL) and uplink (UL) channel measurements in time, angle, and power domains to calculate position estimates based on different techniques. In addition, RAT-external measurements may also be incorporated into the calculation of the user equipment (UE) position, e.g., using UE side sensors such as global navigation satellite system (GNSS) modules [1], [7]. It is expected that Sidelink (UE-to-UE link) [8] and carrier phase measurements [9] will be supported at the latest in 6G.

1) DL and UL Reference Signals: The available signals are Positioning Reference Signal (PRS), Sounding Reference Signal (SRS), Synchronization Signal Block (SSB), and Channel State Information Reference Signal (CSI-RS), with two being newly introduced by rel. 16 as follows. On the one hand, the PRS is a DL signal which may consist of up to 272 resource blocks (RBs). Therefore, up to 400 MHz may be used with the 120 kHz subcarrier spacing (SCS) numerology, although not every orthogonal frequency-division multiplexing (OFDM) subcarrier and symbol of each RB are used by a single BS. This is because the PRS is sent by different BSs and measured by the UE, but with the aim of the least possible interference for improved positioning accuracy. In the time domain, transmissions may be configured with periodic intervals between 4 ms and about 10 s. On the other hand, the rel. 16 SRS is an extension of the existing UL SRS to allow for high-accuracy positioning similar to PRS [7].

2) Measurement Parameters: The high bandwidths at mmWave allow for accurate time measurements. For example, the round-trip time (RTT) between any BS and UE pair is acquired via receiver (RX)-transmitter (TX) time difference measurements along PRS and SRS. It is proportional to the length of the propagation path between, similar to, but more precise than the timing advance (TA) parameter that may be leveraged by enhanced cell ID (E-CID), and can thus be used for positioning. In addition, the absolute distance can be estimated from the reference signal received power (RSRP) following Friis' transmission formula. Contrasting the acquisition of absolute time data, time difference of arrival (TDOA) information, that is proportional to the propagation path length difference between the UE and two BSs, can be leveraged via DL reference signal time difference (RSTD) or UL relative time of arrival (RTOA) measurements. Moreover, the directional communication at mmWaves allows for measurements of transmit and receive angles. Only BS side bearings are used in 5G with the angle of departure (AOD) being the known angle of the BS beam that serves the UE with the best RSRP, whereas the angle of arrival (AOA) of UL signals can be measured directly [11].

3) Standardized Techniques: The UE position is estimated via multilateration and -angulation algorithms. Moreover, there are also hybrid techniques, e.g., *(i)* leveraging both angle and time measurement data, or *(ii)* combining RAT-internal and -external data. Implementations range from non-iterative, i.e., with low delay, to iterative solvers that may achieve higher accuracy. Depending on the used measurements and implementation, the required minimum number of participating BSs differs. The detection of nearby mmWave BSs can be cumbersome due to the need for beam training [11].

B. High-accuracy LCS Performance Requirements

The previously described 5G features provide a complex toolbox for mobile network operators to fulfill the stringent QoS requirements of 5G positioning use cases. Each one can be characterized by one of seven defined SLs considering indoor/outdoor modality, user mobility, and maximum latency, among others [4]. In this work, we focus on the metrics listed in Tab. I, which are compared to initial commercial outdoor rel. 16 requirements and to the ones by 5G Automotive Association (5GAA) (neglecting software update/HD content delivery use cases) and 5G Alliance for Connected Industries and Automation (5G-ACIA). It can be seen that the requirements for higher 2D accuracy (up to ≤ 30 cm) are complemented by increasing minimum availability (up to $\geq$99.9 %), i.e., the ratio between the time in which the positioning service is delivered with the required QoS and the total time. Assuming that UEs do not leave the intended service area, one might

TABLE I
SELECTED OUTDOOR POSITIONING PERFORMANCE REQUIREMENTS.

Reference	Service Level (SL)	Minimum Accuracy	Minimum Availability
3GPP TR 38.855 [12]	regulatory commercial	50.0 m 10.0 m	80.0 %
3GPP TS 22.261 [4]	1	10.0 m	95.0 %
	2	3.0 m	99.0 %
	3	1.0 m	99.0 %
	4		99.9 %
	5	0.3 m	99.0 %
	6		99.9 %
5GAA [6]	minimum maximum	20.0 m 0.1 m	68.3 % 99.7 %
5G-ACIA [13]	-	0.1 m	100.0 %

interpret availability as the ratio of positions from the service area which fulfill the horizontal accuracy requirements, when neglecting the latency requirements et cetera. The 5G-ACIA is even demanding sub-10 cm accuracy without exceptions.

C. Performance in Related Works

Analytical studies [14] and works leveraging channel models [2], [15] show the attainability of mmWave positioning accuracies well below 1 m. However, their transferability to real deployments is questionable. Ray-tracing works provide representative data, but tend to focus on the sub-6 GHz spectrum, e.g., [16]. In [17], combining hybrid time-angle positioning with two mmWave BSs, accuracy better than GNSS is achieved for users traversing a highway, yet the very high mobility scenario does not match with the expected urban mmWave deployments. With regards to measurements, there have been promising indoor studies that achieve high positioning accuracy [18]–[20], but they cannot simply be transferred to outdoor scenarios. The authors in [21] have demonstrated outdoor hybrid positioning with a single mmWave BS, yet the initial results do not meet the performance in the previously discussed works. For all of these studies, the limited number of measurements do not allow for the assessment of service availability which is necessary for the characterization of the attained 3GPP SLs. We have noticed in several works that the error modeling, e.g., in angle and time measurements or for the network-internal time synchronization, is either of limited scope or weakly parametrized [15], [18], if considered at all. Hence, make-or-break requirements for the specified high-accuracy positioning could not be identified either.

III. Methodology

This section first introduces the comprehensive urban mmWave ray-tracing dataset in Sec. III-A which is summarized by Tabs. II and III. Afterward, the considered positioning algorithms are provided in Sec. III-B. Last, Sec. III-B explains the details of the error modeling for the sensitivity analysis.

A. Dataset of an Urban Deployment Scenario

a) Ray-Tracing Simulation: We select a metropolitan setup for the 5G mmWave network deployment, similar to the work [16], as offloading of sub-6 GHz cells is expected in such busy regions. Considering the hostile mmWave domain, central hotspot areas have to be served by multiple cells. We realized a Manhattan grid-like scenario with a total size of 480×480 m in the Altair WinProp software [22]. The urban canyons have a width of 20 m and the quadratic building blocks have a length of 100 m. As shown in Fig. 3, eight BSs operating at 26.5 GHz (n257/n258) and using a fixed equivalent isotropically radiated power (EIRP) of 40 dBm were placed around a central district at the height of 10.0 m. The evaluation area, with a total size of 120×120 m, focuses on one of the adjacent street crossings with 110,000 potential mmWave UE positions in a 20 cm on-street grid at a uniform height of 1.5 m, cf. Tab. II.

The omnidirectional simulation provides ray information between each UE-BS combination which includes signal strength and phase, as well as the underlying transmit/receive azimuth

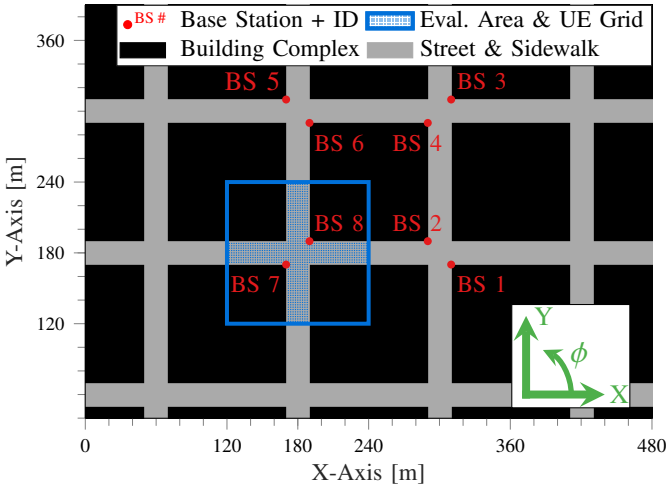

Fig. 3. Urban outdoor deployment of 8 mmWave BSs around central building complex. Directional channel data is available for 110,000 UE positions on a 0.2 m grid within the outlined 120×120 m evaluation area.

(ϕ) and elevation (θ) angles. Therefore, the strongest tap of the channel impulse response (CIR) provides the ideal angle, power, and time measurement data for positioning as there are no distortions, except when the UE is in a non-line-of-sight (NLOS) region. This dataset is used to set the *performance benchmark* and indicated by "perfect angle" or "infinite bandwidth" Channel State Information (CSI).

b) Beam-based Connectivity: To mirror a real mmWave system's behavior, we impose directional antenna pattern characteristics by post-processing using MathWorks MATLAB software [23] as follows. For both sides of the link, either pencil or sector beams, as shown in Fig. 4, are employed, which correspond to using an 8×8 or 4×4 uniform planar array (UPA). In the ideal case, the received signal strength (RSS) is thus increased by the maximum gain of the used beam, i.e. by 19.7 dBi or 13.5 dBi, see Fig. 4. Some rays, however, are suppressed by the beam patterns. In case the RSS drops below −103 dBm, ray data is removed from the directional CIR.

There are infinitely many combinations of how two nodes may orient their antenna beams to connect. Introducing antenna beam codebooks (beambooks) containing a set of beam orientations in the azimuth and elevation plane on either side discretizes the combinatorial problem. Considering the respective HPBWs of 12.8° and 26.3° as depicted in Fig. 4, we choose the spacings of 12° or 24° between the beam-

TABLE II
Dense urban mmWave network dataset parameters.

Parameters	Description and Value
Carrier frequency f_0	26.55 GHz (path loss exponent: 2.6)
EIRP, decoding threshold	40 dBm, −83.5 dBm
Evaluation area	120×120 m
# UE positions	110,000 (0.2 m grid at 1.5 m height)
# BS sites	8 (building corners at 10.0 m height)
Pencil/sector beam gain	19.7 dBi/13.5 dBi
Pencil/sector beam HPBW	12.8°/26.3°
UE beambook ranges	360° azimuth, up to 90° uptilt
BS beambook ranges	270° azimuth, up to 90° downtilt

TABLE III
NUMBER OF BEAM PAIRS BASED ON LEVERAGED UE/BS BEAM TYPES.

	Dataset	*pencil*	*sector*	*mixed*
BS side beambook	**# az. angles**	23	12	23
	# el. angles	8	4	8
UE side beambook	**# az. angles**	30	15	15
	# el. angles	8	4	4
	# Combinations	44,160	2,880	11,040

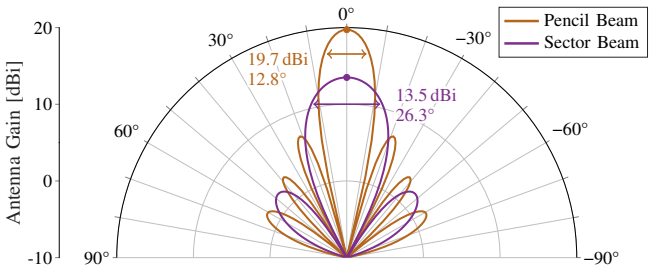

Fig. 4. Boresight beam patterns with maximum gain and HPBW information.

book entries. Regarding the contained elevation angles, the BS side beam orientations cover the range from $\theta_{\text{BS}} \in]-90, 0]\,°$, i.e. there are eight pencil beam elevation angles $\{0, -12, \ldots, -84\}\,°$ and four sector beam elevation angles $\{0, -24, \ldots, -72\}\,°$. On UE side, a similar beambook design uses uptilts instead of downtilts, i.e. $\theta_{\text{UE}} \in [0, 90[\,°$. In the azimuth plane the UEs have to cover all directions such that $\phi_{\text{UE}} \in [0, 360[\,°$. Therefore, there are 30 pencil and 15 sector beam azimuth angles. Last, for the BSs, ϕ_{BS} only covers a 270° range due to building obstruction. Thus, there are 23 and 12 distinct BS beam azimuth angles, respectively. In practice, several antenna panels would be employed to cover such wide angular regions.

In this work, we consider three combinations of UE and BS beam types which result in different numbers of beam pairs as illustrated in Tab. III. When using "pencil" beams on both sides there are $(23 \cdot 8) \cdot (30 \cdot 8) = 44{,}160$ beam pairs, whereas with "sector" beams there are just 2,880. In the third case, "mixed" beam pairs, the BSs use pencil beams whereas the UE uses sector beams. As a consequence, there are 11,040 combinations, cf. Tab. III, each representing an individual channel in the form of a distinct directional CIR.

B. User Positioning Algorithms

This work facilitates the following basic positioning algorithms: We have implemented the non-linear least squares (NLLS)-based iterative multilateration algorithm outlined in [24] that can be used for absolute time and RSS-based positioning. For TDOA-based positioning, we use the non-iterative hyperbolic spherical-interpolation-based method described in [25]. Angle-based user position estimation is realized via the line-of-bearings (LOBs)-based iterative approach in [26].

We also consider the hybrid RAT-internal positioning techniques shown in Fig. 5. Applying the concept from [27] to combine the estimates from separate multiangulation and -lateration algorithms linearly (50/50 %), we realize our first hybrid algorithm, called *"LinComb."* Second, by extending the scheme outlined in [28] from the horizontal plane to 3D space, time and angle information $(\tau_1, \phi_1, \theta_1)$ between a *"single BS"* and UE pair is used efficiently. The third approach is referred to as *"multiple BSs"* and extends the previous approach with time measurements (τ_2, τ_3) to two additional BSs [28].

Moreover, we propose two GNSS-assisted 5G positioning techniques: Comparing the differences between the satellite-based UE position estimate, we adaptively modify the weighting of the LinComb to 25/75 %. Second, the time-based trilateration is adapted to use the GNSS data as the initial position estimate, instead of the center point between the BSs, which is iteratively improved by the NLLS algorithm. The GNSS position estimates are generated following the Gaussian model by [29] with $\mu = 0.34\,\text{m}$ and $\sigma = 0.66\,\text{m}$, which is similar to the recent GNSS performance measurements in [17].

C. Modeling of Sources of Error

Our evaluation of 5G mmWave positioning capabilities is based on the following time and angle error modeling.

a) Beambooks and Angle Estimation: Contrasting the ideal angle knowledge from the simulation baseline, the BS side beambooks result in azimuth and elevation angle measurements being discretized for the DL-AOD technique, i.e., with 12° (pencil) or 24° (sector, mixed) step sizes. Additionally, we consider direct angle measurements by the UL-AOA technique providing better accuracy, i.e., 1° step size for brevity, but angle errors typically fall into a range of several degrees [30].

b) Bandwidth: In real systems, the bandwidth W limits the time resolution in comparison to the infinite bandwidth baseline from simulations. We thus build the complex sums of the CIR taps falling into the intervals with periodicity $1/W$. We consider $W = 100, 200, 400, 800, 1{,}200\,\text{MHz}$ spanning the range from the maximum sub-6 GHz bandwidth to far beyond the ones attained via carrier aggregation in current chipsets.

c) Network Synchronization: Network clock synchronization has to be considered as well because, e.g., UL propagation delay measurements measured by multiple BSs need to be performed simultaneously. Whereas there is a recommendation for large-scale networks to stay below 1,500 ns [31], the authors in [32] propose a 130 ns bound and in [16] 100 ns offsets between the distributed clocks are assumed. GNSS receivers may synchronize BSs to a common clock with sub-10 ns error under clear observation conditions [33], which are not necessarily met by mmWave BSs in the foreseen metropolitan areas. Using so-called network listening [34], a BS may also synchronize by measuring another BS's signals. Wired time synchronization using, e.g., Precision Time

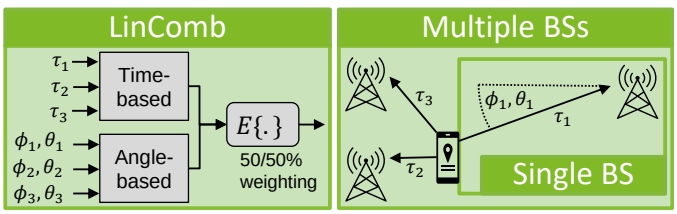

Fig. 5. RAT-internal hybrid positioning with up to three BSs based on absolute time (τ) and BS side azimuth and elevation angle (ϕ, θ) measurements.

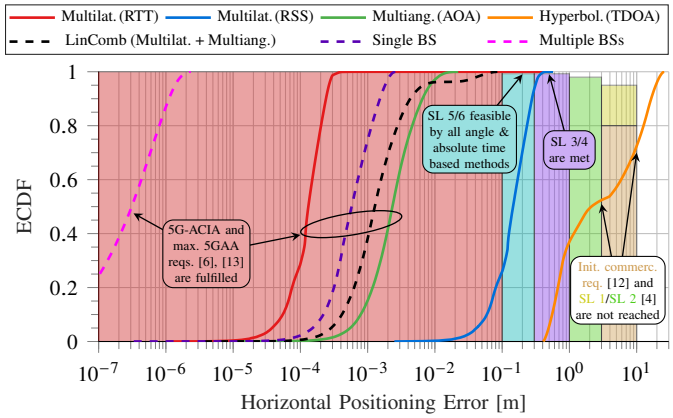

Fig. 6. RAT-internal positioning performance distributions under ideal conditions, i.e., only BSs in LOS as well as no time, angle, and power measurement errors. Dashed lines indicate hybrid time/angle-based positioning.

Protocol (PTP) can reach 1 ns precision [35]. As such, other works on mmWave positioning used values down to 2 ns to 1 ns [15] and 1 ns to 0.25 ns [18], the latter being below the PTP capabilities. With assumptions differing in literature, we aim to derive tolerable errors, i.e., requirements, such that 5G networks may provide the envisioned 3GPP SLs. We use a zero-mean Gaussian error model truncated to $[-\sigma, \sigma]$ [36].

IV. Evaluation

This section evaluates mmWave-based urban outdoor positioning performance. In Sec. IV-A, we first determine the best possible positioning performance for the urban scenario. Second, Sec. IV-B characterizes the impact of time and angle measurements on the attainable positioning SL. At last, hybrid positioning is investigated under non-ideal conditions, chosen based on prior results. The SL characterization in Sec. IV-C also includes the potential of GNSS assistance.

A. Baseline Performance Under Ideal Conditions

Under ideal conditions, 3GPP SLs 4 and beyond are achieved except when using TDOA data, cf. empirical cumulative distribution functions (ECDFs) in Fig. 6. Dropping power measurements from consideration, the highest requirements can be met with absolute time and angle-based methods. Therefore, the new measurements and techniques introduced by 5G rel. 16 are verified to have a higher potential than existing ones. This work now focuses on these five positioning methods under more realistic conditions. We explicitly note that once NLOS measurements are used the high availability requirements of the 3GPP SLs 1 to 6 and by 5G-ACIA cannot be reached anymore; however, some of the use cases specified by 5GAA remain feasible. Thus, suitably dense deployments, probably denser and more costly than for communications only, are needed for sufficient LOS availability in the service area, but also methods are required to detect and avoid degradation from NLOS link opportunities.

B. Sensitivity Analysis of 5G LCS

Contrasting the direct angle measurements in UL AOA, that we assumed to be without error, we now consider the beambook-based impact from using the known azimuth and elevation main lobe angles of the active BSs' beams for the DL AOD technique in Fig. 7. It can be seen that the communication-centric pencil beambook with 12° angle spacings just smaller than the HPBW of the 8×8 UPA cannot enable SL 1 use cases. By moving to a more densely spaced beambook which results in drastically increased beam management overhead but sub-1° azimuth and elevation angle errors, respectively, SLs 1 to 2 are feasible. It must be noted that, in practice, such a densely-spaced beambook results in a higher likelihood for erroneous beam selection, and such, larger errors may be incurred. Assuming the use of a hybrid/digital beamforming architecture at the BSs, direct AOA estimation in the UL could naturally enable higher service levels. This comes at increased hardware costs and energy consumption.

Moving on to the impact of the leveraged signaling bandwidth on time measurements-based positioning, as shown in Fig. 8. It can be seen that 100 MHz suffice for SL 1 use cases, with 200 MHz barely failing to meet SL 2 requirements. They can, however, be met when using 400 MHz. Using carrier aggregation, SL 3 is barely met with 800 MHz, yet SL 4 is narrowly missed even with 1,200 MHz bandwidth. Considering other impairments, we recommend the use of at least 200 MHz for SL 1, 400 MHz for SL 2, and 1,200 MHz for SL 3. Higher SL categories require even more bandwidth with aggregation up to 2.4 GHz already standardized [37] and more expected for 6G. Potentially 5G NR Unlicensed (NR-U) in frequency range 2 (FR2) band n263 has to be used

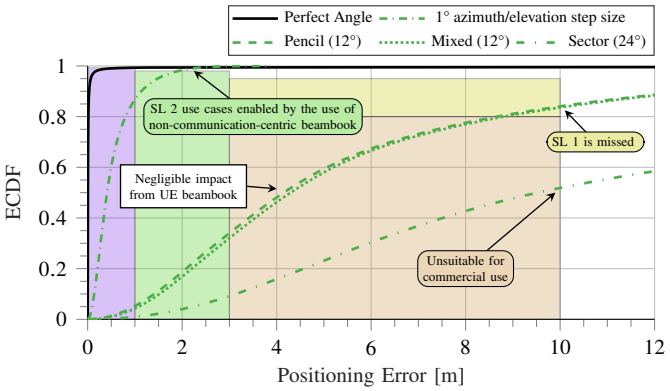

Fig. 7. Positioning error incurred by triangulation for different UE-BS beambook combinations compared to the perfect angle-based performance.

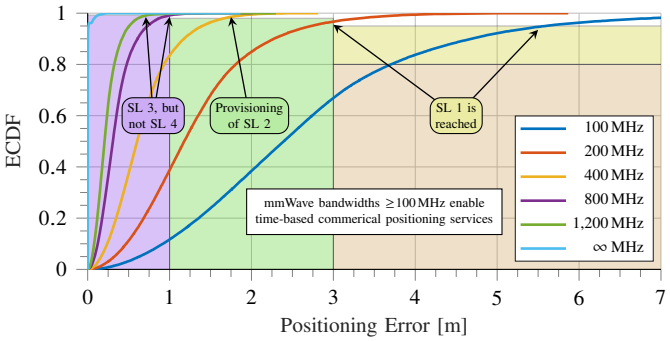

Fig. 8. Trilateration for different positioning signaling bandwidths compared to ideal conditions. Incurred horizontal positioning errors depicted by ECDF.

TABLE IV
RECOMMENDED NETWORK TIME SYNCHRONIZATION REQUIREMENTS FOR DIFFERENT POSITIONING SERVICE LEVELS.

Ref.	Service Level (SL)	Positioning Requirements (Accuracy @ Availability)	Tolerable Time Asynchronicity
[12]	commercial	10.0 m @ 80.0 %	< 20 ns
[4]	1	10.0 m @ 95.0 %	< 11 ns
	2	3.0 m @ 99.0 %	< 2 ns
	3/4	1.0 m @ 99.0/99.9 %	< 0.5 ns
	5/6	0.3 m @ 99.0/99.9 %	</≪ 0.25 ns
[6]	maximum	0.1 m @ 99.7 %	≪ 0.25 ns
[13]	-	0.1 m @ 100.0 %	≪ 0.25 ns

due to support for non-aggregated cell bandwidths of up to 2 GHz [37]. However, operation in the unlicensed spectrum is sub-optimal when aiming to achieve beyond 99 % availability.

At such broad bandwidths the synchronization errors between the network's BSs obtain a higher influence, by far exceeding the impact of the signaling bandwidth. In contrast to the previous evaluation, Tab. IV summarizes our experiments to determine what levels of asynchronicity can be tolerated so that commercial positioning services remain feasible. While the initial commercial 3GPP requirements need network synchronization in the sub-20 ns range which can be attained via PTP and GNSS [33], [35], this is by orders of magnitude stricter than the typical design requirements for mobile networks (1,500 ns) [31]. For SL 1 the required synchronization of below 11 ns is in the range of GNSS time synchronization under clear conditions. As such, higher-order SLs need to switch to a wired synchronization, e.g., using PTP. However, the SLs 3 to 6 require below-1 ns synchronization, particularly when further considering signaling bandwidth-based errors. This is not even guaranteed by PTP [35]. As such, 5G network time synchronization is currently the limitation when aiming for time-based high-accuracy positioning. Considering that time-sensitive networking (TSN) has emerged as a hot topic for mission-critical services in 5G and beyond networks [38], this problem could be fixed by future 3GPP standardization.

C. On the Potential of Hybrid Positioning

In the following section, we consider the gains of using hybrid positioning techniques over non-hybrid techniques. Based on the previous evaluation, our investigation uses a communication-centric beambook (12°) for DL AOD measurements of BS azimuth and elevation angles which we previously showed is not sufficient to attain SL 1 via triangulation. Due to time synchronization errors having a much larger impact than the channel impact, we further consider network asynchronicity errors. Here, we use 11 ns which is just good enough to attain SL 1 via trilateration. These two classifications are confirmed by the respective violins in Fig. 9. We note that the better performance of trilateration over triangulation only holds for the previously described error modeling.

We now consider RAT-internal hybrid positioning. Determining the mean of the trilateration and -angulation results, LinComb falls into SL 1 and comes with an increased accuracy against trilateration. Moreover, the tail of the distribution with very high errors is truncated. Moving on to the "multiple BSs" algorithm, SL 1 is missed with the 95 % confidence interval of about 13 m ranging between the ones of trilateration and -angulation (9.9, 14.9 m), however, the tail is shortened. Dropping the two non-serving BSs from consideration, the position estimates of the "single BS" are clearly in the SL 1 range with mean and median errors of about 2.1 m and a 95 % confidence interval of 5.4 m, cf. Fig. 9. This is an unexpected improvement over the "multiple BSs" approach, cf. Fig. 6. The reason is that network time synchronization is irrelevant as just one BS is performing the time measurements. Hence, this algorithm underlines the high potential of hybrid positioning as the TSN problem is avoided, cf. Sec. IV-B, whereas the resource efficiency (energy consumption, spectral resources) is increased. Further, excessive per-BS mmWave beam training overhead, which is incurred before positioning, is minimized.

We now assess the gains of using GNSS for assistance, as proposed in Sec. III-B. Using the position provided by GNSS as the starting point of the iterative trilateration algorithm, the mean accuracy is improved a little from 3.95 m to 3.59 m, with the improvement of the 95 % confidence interval being more noticeable from 9.88 m to 8.98 m. Similarly, the distribution tail is shortened. This characteristic will be useful when aiming to provide the highest SLs. It can also be observed when using the GNSS estimate to change the weighting of the LinComb algorithm from 50/50 % to 25/75 %. Overall, the GNSS-aided LinComb algorithm, which combines three BSs' time and angle measurements with GNSS, performs second best (mean error: 3.0 m, 95 % confidence interval: 7.4 m) and is only beaten by the resource efficient single BS-based approach which avoids the network time synchronization issue.

Hence, in this section we have shown that hybrid positioning using RAT-internal measurements can provide a significantly better performance and that RAT-external estimates, such as by GNSS modules and processed according to our proposed algorithms, are helpful in the further mitigation of outlier positioning errors. Both are needed for SLs 2-6 aiming for 3.0 m to 0.3 m accuracy at beyond 99.0 % availability. As such, RAT-native sensor information acquired by 6G joint communication and sensing (JCAS) will be highly valuable for user positioning.

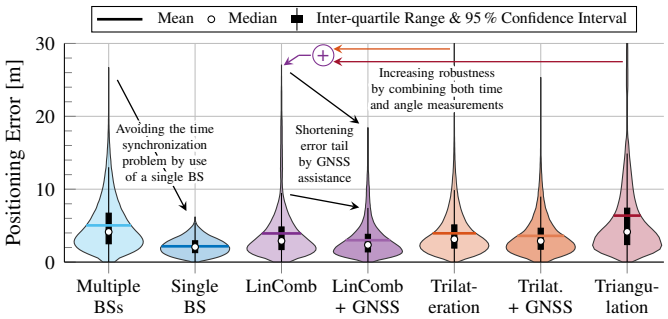

Fig. 9. Performance of hybrid positioning, with and without GNSS assistance, under harsh conditions. Here: 11 ns network time asynchronization and pencil beam-based angle information with 12° resolution.

V. Conclusions

In this work, we classified the performance of 5G mmWave outdoor positioning according to the 3GPP-defined service levels (SLs). We showed that SLs 1 to 3 can be met under LOS conditions by absolute time-based multilateration and -angulation, respectively, if more than 800 MHz bandwidth or angle estimators with sub-1° accuracy are used. Therefore, most but not all of the 5GAA's use cases in the scope of future ITSs are feasible. However, we further identified network time synchronization as a critical limitation for time-based positioning. Depending on the desired SL, time synchronization between BSs has to be smaller than 11 ns to 0.25 ns, with sub-ns synchronization exceeding the limits of current protocols such as PTP. This ought to be addressed further moving towards 6G networks for high-accuracy positioning and sensing services.

We further studied hybrid positioning. By combining the two estimates of the multilateration and multiangulation techniques, the positioning becomes more robust. Further, user positioning with time and angle measurements from just the single serving BS is particularly promising because it avoids the problem of time synchronization and increases resource efficiency before and during positioning. Finally, by including GNSS as a RAT-external sensor, as foreseen in 5G for outdoor users such as pedestrians and vehicles, we have shown that the positioning service availability is further enhanced by our proposed techniques. Therefore, while 5G mmWave positioning is highly capable, the beyond 99 % availability goals of the strictest SLs are better met with assistive external data.

In our future works, we will investigate mmWave hybrid positioning for mobile UEs with a focus on latency and characterize the positioning-specific spectral resource overhead.

Acknowledgment

This work has been partly funded by the German Federal Ministry of Education and Research (BMBF) in the course of the *6GEM Research Hub* under grant number 16KISK038 and by the Ministry of Economic Affairs, Industry, Climate Action and Energy of the State of North Rhine-Westphalia (MWIKE NRW) along with the *Competence Center 5G.NRW* under grant number 005-01903-0047.

References

[1] S. M. Razavi *et al.*, "Positioning in cellular networks: Past, present, future," in *IEEE Wirel. Commun. and Netw. Conf. (WCNC)*, Apr. 2018.

[2] S. Dwivedi *et al.*, "Positioning in 5G networks," *IEEE Commun. Mag.*, vol. 59, no. 11, pp. 38–44, Nov. 2021.

[3] R. Keating *et al.*, "Overview of positioning in 5G New Radio," in *Int. Symp. on Wirel. Commun. Syst. (ISWCS)*, Aug. 2019.

[4] 3GPP TS 22.261 v19.9.0, "TSG SA; service requirements for the 5G system; stage 1 (release 19)," Sep. 2022.

[5] 3GPP TR 22.872 v16.1.0, "TSG SA; study on positioning use cases; stage 1 (release 16)," Sep. 2018.

[6] 5G Automotive Association (5GAA). (2021, Feb.) System architecture and solution development; high-accuracy positioning for C-V2X. Technical Report, v1.0. Last accessed: 2022-12-23. [Online]. Available: https://5gaa.org/wp-content/uploads/2021/02/5GAA_A-200118_TR_V2XHAP.pdf

[7] L. Xingqin and L. Namyoon, *5G and Beyond: Fundamentals and Standards*, 1st ed. Springer International Publishing, Mar. 2021.

[8] 3GPP. Work plan. Version December 12th 2022. Last accessed: 2022-12-23. [Online]. Available: https://3gpp.org/ftp/Information/work_plan

[9] S. Fan *et al.*, "Carrier phase-based synchronization and high-accuracy positioning in 5G New Radio cellular networks," *IEEE Trans. on Commun.*, vol. 70, no. 1, pp. 564–577, Jan. 2022.

[10] 3GPP TS 38.305 v17.2.0, "TSG RAN; stage 2 functional specification of UE positioning in NG-RAN (release 17)," Sep. 2022.

[11] E. Dahlman, S. Parkvall, and J. Sköld, *5G NR: The Next Generation Wireless Access Technology*, 2nd ed. Academic Press, Sep. 2020.

[12] 3GPP TR 38.855 v16.0.0, "TSG RAN; study on NR positioning support (release 16)," Mar. 2019.

[13] 5G Alliance for Connected Industries and Automation (5G-ACIA). (2019, Feb.) 5G for connected industries and automation. White Paper, 2nd ed. Last accessed: 2022-12-23. [Online]. Available: https://5g-acia.org/wp-content/uploads/2021/04/WP_5G_for_Connected_Industries_and_Automation_Download_19.03.19.pdf

[14] H. Wymeersch *et al.*, "5G mmWave positioning for vehicular networks," *IEEE Wirel. Commun.*, vol. 24, no. 6, pp. 80–86, Dec. 2017.

[15] F. Lemic *et al.*, "Localization as a feature of mmWave communication," in *Int. Wirel. Commun. and Mob. Comput. Conf. (IWCMC)*, Sep. 2016.

[16] M. Koivisto *et al.*, "Joint device positioning and clock synchronization in 5G ultra-dense networks," *IEEE Trans. on Wirel. Commun.*, vol. 16, no. 5, pp. 2 866–2 881, Mar. 2017.

[17] S. Saleh *et al.*, "Would future mmWave wireless networks be an alternative positioning technique to GNSS-based high precision positioning?" in *IEEE Vehicular Tech. Conf. (VTC-Spring)*, Jun. 2022.

[18] O. Kanhere *et al.*, "Map-assisted millimeter wave localization for accurate position location," in *IEEE Global Commun. Conf. (GLOBECOM)*, Dec. 2019.

[19] G. Yammine *et al.*, "Experimental investigation of 5G positioning performance using a mmWave measurement setup," in *Conf. on Indoor Positioning and Indoor Navigation (IPIN)*, Dec. 2021.

[20] K. Heimann, J. Tiemann, S. Böcker, and C. Wietfeld, "Cross–bearing based positioning as a feature of 5G millimeter wave beam alignment," in *IEEE Vehicular Tech. Conf. (VTC2020-Spring)*, May 2020.

[21] Y. Ge *et al.*, "Experimental validation of single base station 5G mmWave positioning: Initial findings," in *IEEE Conf. on Inf. Fusion (FUSION)*, Jul. 2022.

[22] Altair Engineering Inc. Altair WinProp. [Online]. Available: www.altair.de/resource/altair-winprop-datasheet (Accessed 2022-12-23).

[23] The MathWorks Inc. Phased array system toolbox. [Online]. Available: www.mathworks.com/products/phased-array (Accessed 2022-12-23).

[24] Y. He and A. Bilgic, "Iterative least squares method for global positioning system," *Adv. in Radio Science*, vol. 9, pp. 203–208, Aug. 2011.

[25] J. Smith and J. Abel, "Closed-form least-squares source location estimation from range-difference measurements," *IEEE Trans. on Acoustics, Speech, and Signal Proc.*, vol. 35, no. 12, pp. 1 661–1 669, Dec. 1987.

[26] A. Pages-Zamora, J. Vidal, and D. H. Brooks, "Closed-form solution for positioning based on angle of arrival measurements," in *IEEE Symp. on Personal, Indoor and Mob. Radio Commun. (PIMRC)*, Sep. 2002.

[27] A. Sayed, A. Tarighat, and N. Khajehnouri, "Network-based wireless location: challenges faced in developing techniques for accurate wireless location information," *IEEE Signal Proc. Mag.*, vol. 22, no. 4, pp. 24–40, Jun. 2005.

[28] V. Y. Zhang *et al.*, "Hybrid TOA/AOA-based mobile localization with and without tracking in CDMA cellular networks," in *IEEE Wirel. Commun. and Netw. Conf. (WCNC)*, Jul. 2010.

[29] A. El Abbous and N. Samanta, "A modeling of GPS error distributions," in *European Navigation Conf. (ENC)*, May 2017.

[30] J. Tiemann, O. Fuhr, and C. Wietfeld, "CELIDON: Supporting first responders through 3D AOA-based UWB ad-hoc localization," in *Int. Conf. on Wirel. Mob. Comput., Netw. and Commun. (WiMob)*, Oct. 2020.

[31] ITU-T G.8271.1/Y.1366.1 (2020) – Amendment 2, "Network limits for time synchronization in packet networks with full timing support from the network," Feb. 2022.

[32] H. Li *et al.*, "Analysis of the synchronization requirements of 5G and corresponding solutions," *IEEE Commun. Standards Mag.*, vol. 1, no. 1, pp. 52–58, Mar. 2017.

[33] K. F. Hasan, Y. Feng, and Y.-C. Tian, "GNSS time synchronization in vehicular ad-hoc networks: Benefits and feasibility," *IEEE Trans. on Intell. Transp. Syst.*, vol. 19, no. 12, pp. 3 915–3 924, Mar. 2018.

[34] 3GPP TR 36.922 v17.0.0, "TSG RAN; E-UTRA; TDD home eNodeB (HeNB) RF requirements analysis (release 17)," Mar. 2022.

[35] IEEE Std 1588-2019, "Precision clock synchronization protocol for networked measurement and control systems," Jun. 2020.

[36] I. Müürsepp *et al.*, "Performance evaluation of 5G-NR positioning accuracy using time difference of arrival method," in *IEEE Int. Mediterranean Conf. on Commun. and Net. (MeditCom)*, Sep. 2021.

[37] 3GPP TS 38.101-2 v17.7.0, "TSG RAN; UE radio transmission and reception; part 2: Range 2 standalone (release 17)," Sep. 2022.

[38] F. Kurtz, G. Stomberg, M. B. Bandeira, J. Püttschneider, F. Greiwe, M. Kaupmann, C. Hams, T. Harnisch, M. O. Tay, A. Choudhary, J. R. Trevino, A. Bhanderi, A. Rajashekbhar, P. Vemana, A. Alhanalfi, T. Faulwasser, and C. Wietfeld, "Software-defined networking driven time-sensitive networking for mixed-criticality control applications," in *Int. Conf. on Inf. and Commun. Tech. Convergence (ICTC)*, Oct. 2022.